

Modelling of batch biomethanation process for maximizing income based on values of consumed and produced gases

Seyed Ali Jafari*, Shahriar Osfouri*,†, and Reza Azin**

*Department of Chemical Engineering, Faculty of Petroleum, Gas, and Petrochemical Engineering, Persian Gulf University, Bushehr, Iran

**Department of Petroleum Engineering, Faculty of Petroleum, Gas, and Petrochemical Engineering, Persian Gulf University, Bushehr, Iran

(Received 12 September 2019 • accepted 31 January 2020)

Abstract—Economic estimation of an environmental-friendly biomethanation process based on economic values of consumed and produced gases would be a unique attitude. In this paper, time and space dependent concentration profiles of components involved in a batch process, designed for biomethanation, were predicted through a mass transfer modelling. The reaction terms used in the modeling required bio-kinetic parameters of μ_{max} , m , k_L , $Y_{C/L}$, $Y_{X/L}$, and $Y_{P/L}$ which were globally optimized via a predefined algorithm using some experimental data as 0.0987 day^{-1} , 0.1374 day^{-1} , $1.5422 \text{ mole m}^{-3}$, -1.3636 , -0.0183 , -0.0908 . Upon model verification, process income was calculated for a long-term scenario under a variety of factors and maximized through response surface methodology. The maximum income achieved was $\$-0.4/\text{m}^3$ bioreactor. A term carbon subsidy was considered in the income equation in order to find a break-even income for subsidy value of $\$363/\text{ton CO}_2$. Sensitivity analysis revealed that the amount of carbon subsidy directly influenced the selection of low or high levels of some process parameters to make the process profitable. In addition, it was found that pressure and liquid volume were the most important factors to achieve maximum income when $\$30$ and $\$300/\text{ton CO}_2$ carbon subsidy were allocated to the process, respectively.

Keywords: Biomethanation, Methanogens, Mass Transfer Modeling, Kinetic, Greenhouse Gas

INTRODUCTION

CO_2 gas, due to thermodynamically low energy value, is considered as a low-efficient component which has potential to be converted to useful products on condition that high energy under harsh conditions is applied to the system [1]. On the other hand, this greenhouse gas (GHG) has led to global warming disaster because of the uncontrollable emission over the last 100 years of fossil fuel consumption [2]. The largest part of GHGs emissions belongs to CO_2 (73%), followed by CH_4 (18%), N_2O (6%), and F-gases (3%) [3,4]. Such a terrible trend concerns scientists to offer attractive and environmental-friendly technologies for convincing governments to reduce emissions. On this basis, some incentive and penalty regulatory policies such as carbon cap-and-trade were proposed to industries around the world aimed at persuading them for substitution of their fossil fuels with renewable ones [5]. According to British Petroleum (BP) Statistical Review of World Energy, the share of renewables in global power generation increased from 7.4% to 8.4% in 2017, which is a green light to the fulfillment of the goal [4]. Besides, converting CO_2 in flue gases of combustion processes into more valuable substances facilitates decreasing its concentration in the atmosphere [2,6]. Utilizing CO_2 would be an attractive possibility for scientists to work on more because CO_2 is a carbon-based

material that potentially can be a substitute for carbon-based fossil fuels [6].

Power to gas (P2G), a chemical storage of electricity in gas grid, is a technology that provides both a clean environment as well as green fuel that simultaneously supports carbon neutralization. This technology has many advantages over other conventional storage methods in terms of capacity and costs [7-9]. If methane gas is considered as the final gaseous product, CO_2 will be utilized along with H_2 via Sabatier reaction. Also, methane is much more compatible with the existing infrastructure for injection into the natural gas grid rather than other probable products such as hydrogen [2,10]. In this regard, biological approaches using methanogens for methane production are preferred due to environmental friendly nature and performing the process under moderate environmental conditions (temperature less than 70°C and pressure about 1 atm) [11]. Furthermore, methanogens have less sensitivity to impurities in the input gases to the biomethanation process in comparison with catalysts in chemical methanation [12]. However, biological approaches suffer from slow kinetics [13]. The biomethanation process would be more attractive when in-situ methane production and long-term storage in an underground natural gas reservoir, as a natural bioreactor, are the main goals. It is a unique and challenging issue that seems to be the future of our energy [14]. Although there are many studies published on the biomethane production concurrent with CO_2 removal under variety of strategies such as continuous stirred-tank reactor (CSTR) [12], plug [15], batch [16], semi-batch [17], fixed-bed [11,18], and trickle-bed [19], a bioreactor with batch strat-

†To whom correspondence should be addressed.

E-mail: osfourir@pgu.ac.ir

Copyright by The Korean Institute of Chemical Engineers.

egy seems to match more with the concept of the in-situ biomethane production in a natural underground reservoirs.

Scientists, with the aid of mathematical modeling, try to overcome experimental works limitations. Engineering simulation of a bioreactor enables researchers to predict the process performance in a broader operational ranges without doing any experimental work, minimize expenses and expedite development [12]. Process prediction would be difficult in biological approaches due to unpredictable behavior of living organisms. So, researchers mostly prefer to focus on hydrodynamic of an anaerobic fermentation [20]. Nonetheless, there are several modeling and simulation studies published on achieving gas-liquid mass transfer coefficient in biomethanation bioreactors, which is of great importance to scale up a bio-process [12]. Bensmann et al. developed a mathematical model within a rising bubble reactor served for methanation of hydrogen [21]. Leonzio used ChemCad software to simulate a biomethanation process followed by an optimization study using response surface methodology (RSM) for investigating the effect of operational factors on methane evolution rate [22]. A dynamic model for a CSTR was developed by Inkeri et al. with the aim of gas-liquid mass transfer prediction with a novel approach that combines semi-fundamental modeling of gas-liquid mass transfer, hydrodynamics, and biological reactions [12].

In the present study, a time and space-dependent mathematical mass transfer modeling was developed in both gas and liquid phases to predict the rate of CH₄ production, CO₂ and H₂ consumption, and microorganism growth over time and length of the bioreactor working under a batch strategy. The main concern of the current modeling was maximizing process income calculated through a provided equation based on the economic values of input and output gases to the studied bioreactor. Although there are several published literature on economic evaluation of a biomethanation process, the approach used for calculating income was not previously addressed. This approach is considered as a novel part of the manuscript. To have a reliable modelling result, six unknown bio-kinetic parameters of the microorganism were achieved by fitting the kinetic model with published experimental data and then globally optimized through a predefined algorithm for extending to the whole range of experimental conditions. Then, the finalized kinetic parameters were implemented within the mass transfer model for prediction of concentrations of CH₄, CO₂, H₂, and biomass in both gas and liquid phases. After model verification, RSM was employed as a powerful tool for optimization to find the maximum income under the best combination of four independent factors, including temperature, pressure, the mole ratio of H₂/CO₂, and percentage of saturated concentrations (PSC) of H₂ and CO₂ in the liquid phase. Finally, a sensitivity analysis was performed to have a profound insight into the income when undergoes changes in the amount of carbon subsidy as well as operational conditions. This part of study can also be considered as another novelty of the present research work.

METHODOLOGY

To predict concentrations of CH₄, H₂, CO₂ and biomass throughout time and length of the studied batch bioreactor, a mathemati-

cal modeling was developed. The required unknown bio-kinetic parameters for reliable substitution of respective reaction rates into the developed mass transfer model were obtained via fitting kinetic models with some experimental data collected from literature [23]. A predefined algorithm served to optimize a set of kinetic parameters and extend them to the whole ranges of experimental conditions. Finalized parameters in this way are called globally optimized parameters [24]. At the end, RSM was utilized to maximize the calculated income based on the amount of consumed and produced gaseous components.

1. Kinetic Reactions

Biomethanation is produced by the reaction noted in Eq. (1) and supported by the following kinetic reactions, Eqs. (2) to (5), that were adjusted as a linear expression of H₂ consumption rate, r_{H_2} .



$$r_{H_2} = (q_L^{max} C_L) C_x / (C_L + k_L) \quad (2)$$

$$r_X = Y_{X/L} (r_{H_2} - m C_x) \quad (3)$$

$$r_C = - \left[Y_{C/L} r_{H_2} + \left(\frac{1}{4} - Y_{C/L} \right) m C_x \right] \quad (4)$$

$$r_P = \left[Y_{P/L} r_{H_2} + \left(\frac{1}{4} - Y_{P/L} \right) m C_x \right] \quad (5)$$

where q_L^{max} is maximum H₂ consumption and is calculated using Eq. (6). C_x and C_L are biomass and hydrogen concentrations in the liquid phase, respectively, which are simultaneously calculated and substituted via Eq. (14). Also, k_L and m are saturation constant and maintenance coefficient, respectively. The yields $Y_{i/L}$ are theoretical maximal (C)-molar yields which are written on the basis of limiting substrate, hydrogen. Besides, r_C and r_P are CO₂ consumption and CH₄ production rates, respectively. The maximum H₂ consumption is defined as follows:

$$q_L^{max} = (1/Y_{X/L}) \mu_{max} + m \quad (6)$$

where μ_{max} is the maximum growth rate of biomass.

Because of a variety of investigated experimental conditions in the reference literature, different sets of kinetic parameters of μ_{max} , m , k_L , $Y_{C/L}$, $Y_{X/L}$, and $Y_{P/L}$ are inevitably obtained under each of respective conditions. To have a fixed set of parameters extending to the whole range of experimental conditions, a predefined algorithm was developed to globally optimize each of the kinetic parameters (data unpublished).

2. Mass Transfer Simulation

A schematic of a serum bottle, as the studied bioreactor, is depicted in Fig. 1. It is a cylindrical vessel that initially contains specific amount of liquid, a culture medium inoculated with methanogens, as well as gaseous substrate on top of it. The gaseous substrate contains CO₂ and H₂ with defined mole ratios of 1:1 or 4:1 which is injected into the bioreactor to attain a fixed pressure of 50 or 100 atm. Gaseous substrates gradually diffuse and dissolve into the liquid phase and are consumed by microorganisms to produce biomethane. CH₄ is generated in the liquid phase and diffuses back in the gas phase. According to the reference literature, the liquid phase of the bioreactor was initially saturated with gaseous substrates. However, other possible soluble concentrations as a percentage of saturated

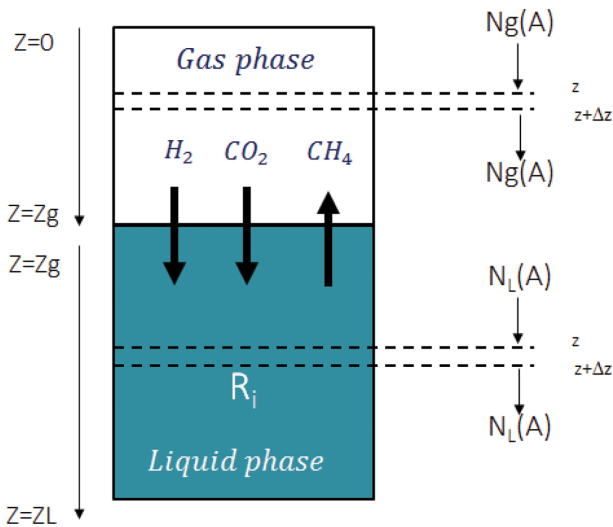


Fig. 1. Schematic for the studied batch bioreactor.

concentrations (PSC) were also investigated.

If convection and dispersion are assumed negligible, a one-dimensional molecular diffusion governs the internal flux to the liquid and gas surfaces. Two different sets of governing equations were developed separately for gas and liquid phases, which led to simultaneous calculation of concentrations of four components (H₂, CO₂, CH₄ and biomass) in both phases. This can be considered as another highlight part of the research work. The gas phase was presumed as a concentrated mixture of CO₂, H₂, and CH₄. The governing equation for gas phase is written as Maxwell-Stefan equation as a function of time and space as shown in Eq. (7).

$$\frac{\partial \rho \omega_i}{\partial t} + \nabla \cdot (\rho \omega_i \mathbf{u} - \rho \omega_i \sum_j \bar{D}_{ij} (\nabla y_j + (y_j - \omega_j) \frac{\nabla P}{P}) - D_i^T \frac{\nabla T}{T}) = 0 \quad (7)$$

The initial and boundary conditions to Eq. (7) for the whole gaseous participants, i.e., CO₂, H₂, and CH₄, are written as follows:

@ z = 0 for CO₂, CH₄ and H₂:

$$\frac{\partial C_{g,i}}{\partial z} = 0, \text{ No flux} \quad (8)$$

@ z = z_g for i = CO₂ or H₂:

$$N_{g,i} = N_{L,i} = D_{L,i} \frac{((C_{g,s,i}/H_{r,i}) - C_{L,s,i})}{\Delta z} \quad (9)$$

$$\text{for CH}_4: N_g = N_L = D_{eff,i} \frac{((C_{L,s,i} \cdot H_{r,i}) - C_{g,s,i})}{\Delta z} \quad (10)$$

@ t = 0 for i = CO₂ and H₂:

$$C_{g,i} = \text{constant} \quad (11)$$

$$\text{for CH}_4: C_{g_{mi}} = \text{zero} \quad (12)$$

where ρ , \bar{D}_{ij} , y_j , ω_j , N_g , N_L , $C_{g_{mi}}$, $C_{g_{ss}}$ and $C_{L,s}$ are the mixture density, multicomponent Fick diffusivity, mole and mass fractions of the j^{th} component, gas and liquid diffusive fluxes, initial concentrations of i^{th} component in gas phase and concentrations in gas and liquid phases near the interface, respectively. Δz measures a tiny dis-

tance below or above the interface in each of the phases. i and j refer to components involved in the process, i.e., CO₂, H₂, and CH₄, which j refers to components in gas phase rather than i . Gas and liquid concentrations are calculated via Eq. (7) and Eq. (14), respectively. Besides, u , D_i^T , ∇P , and ∇T are assumed zero in the present study and referred to as velocity, thermal diffusion coefficient, pressure, and temperature gradients, respectively. Diffusivity coefficients of gases in liquid phase, $D_{L,i}$ were substituted from literature and interpolated as a function of water viscosity variations under different ranges of temperature and pressure according to data reported by Hayduk and Laudie [25]. Eqs. (9) and (10) inferred the equality of molar flux in the gas and liquid interface. The effective diffusion coefficient of methane in gas mixture, $D_{eff,i}$ was derived from Eq. (13) for multicomponent gas mixtures, as follows [26]:

$$D_{eff,i} = \frac{1 - y_i}{\sum_j \frac{y_j}{D_{ij}}} \quad (13)$$

where D_{ij} is diffusion coefficient of pair gases at different temperature and pressures derived from either correlations suggested in literature [27] or interpolating data reported by other researchers [28,29]. Henry's constant, H_r , is determined as a function of temperature and vapor pressure of the solvent for each of the studied gas components separately [30].

For the liquid phase, the governing equation can be suggested to follow Fick's Law due to the presence of a solvent, water, in this phase. Therefore, Eq. (14) is developed for soluble components as well as biomass in the liquid phase.

$$D_{L,i} \frac{\partial^2 C_{L,i}}{\partial z^2} \pm r_i = \frac{\partial C_{L,i}}{\partial t} \quad (14)$$

The initial and boundary conditions to Eq. (14) are as:

$$\text{@ } z = z_g \text{ for } i = \text{CO}_2, \text{H}_2 \text{ and CH}_4: N_{g,i} = N_{L,i} \quad (15)$$

$$\text{for biomass: } \frac{\partial C_L}{\partial z} = 0 \quad (16)$$

$$\text{@ } z = z_L \text{ for } i = \text{CO}_2, \text{H}_2, \text{biomass and CH}_4: \frac{\partial C_{L,i}}{\partial z} = 0 \quad (17)$$

$$\text{@ } t = 0 \text{ for } i = \text{CO}_2 \text{ and H}_2: C_{L_{mi}} = C_{g_{mi}}/H_{r,i} \text{ (saturated conc.)} \quad (18)$$

$$\text{for biomass: } C_{L_{mi}} = \text{constant} \quad (19)$$

$$\text{for CH}_4: C_{L_{mi}} = \text{zero} \quad (20)$$

where C_L is time and space dependent concentration of a given component in the liquid phase. r_i values are substituted from the corresponding Eq. (2) to Eq. (5).

If the initial concentrations of gaseous substrates, CO₂ and H₂, in the liquid phase are considered as a proportion of saturation, PSC, a more real scenario arises and the corresponding initial condition in the liquid phase, Eq. (18), is expressed as Eq. (21). The governing equation and corresponding boundary conditions used for liquid phase, Eqs. (14)-(20), remain unchanged.

$$\text{@ } t = 0 \text{ for CO}_2 \text{ and H}_2: C_{L_{mi}} = b \cdot (C_{g_{mi}}/H_{r,i}) \quad (21)$$

where b is percentage value, a number between 0 and 1.

3. Process Optimization for Maximizing Income

To find the significance of some studied factors as well as their interactions on maximizing income, a powerful statistical tool as RSM is used. In the present study, the developed mathematical model is used to make a proper estimation of the substrate consumption and methane production over time. An equation for process income quantification, as the main response, is introduced as Eq. (22).

$$\text{Response (Income)} = \text{CH}_4 \text{ price} + \text{CO}_2 \text{ Tax} - \text{H}_2 \text{ cost} - \text{CO}_2 \text{ capture Cost} \quad (22)$$

All the terms used in Eq. (22) are in USD and are calculated based on the volume of the studied bioreactor. The term CO₂ Tax is considered here as a reward or subsidy from the government to carbon utilizers in a biomethanation plant in line with environmental policies. Actually, this value can be assumed at least equal to the tax dedicated on CO₂ emissions in a specific country that should be paid by CO₂-producing companies to the government. To persuade the private sector to invest in the biomethanation process, defining the minimum subsidy to meet break-even income can be effective.

The effect of four different factors, as listed in Table 1, is stud-

Table 1. Studied factors and their corresponding levels designed via CCD

Independent factor	Symbol	Level				
		$-\alpha$	-1	0	+1	$+\alpha$
Temperature (K)	A	305	317.5	330	342.5	355
Pressure (atm)	B	50	75	100	125	150
H ₂ /CO ₂	C	0.25	1.5	2.75	4	5.25
PSC	D	0	15	30	45	60

Table 2. Globally optimized kinetic parameters

Kinetic parameters	Value
μ_{max} (day ⁻¹)	0.09872
k_L (mol m ⁻³)	1.54222
m (day ⁻¹)	0.13740
$Y_{X/L}$	-0.01830
$Y_{C/L}$	-1.36359
$Y_{P/L}$	-0.09077

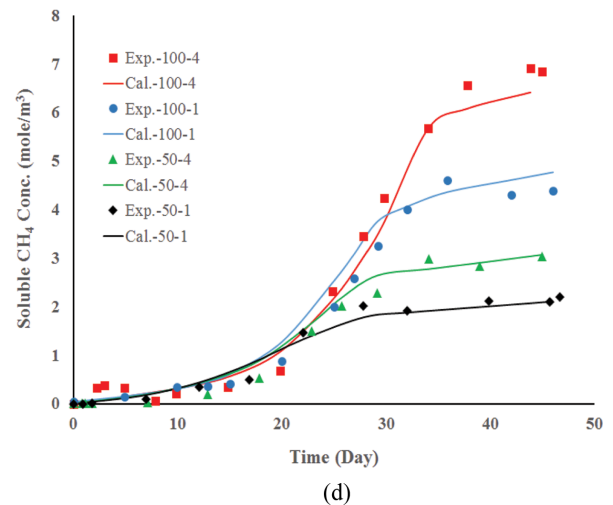
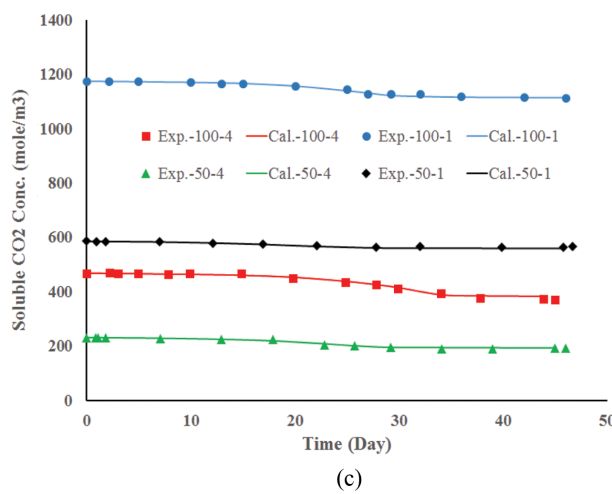
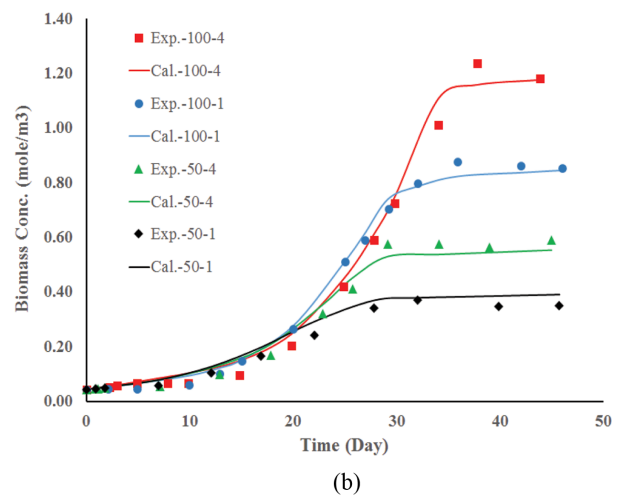
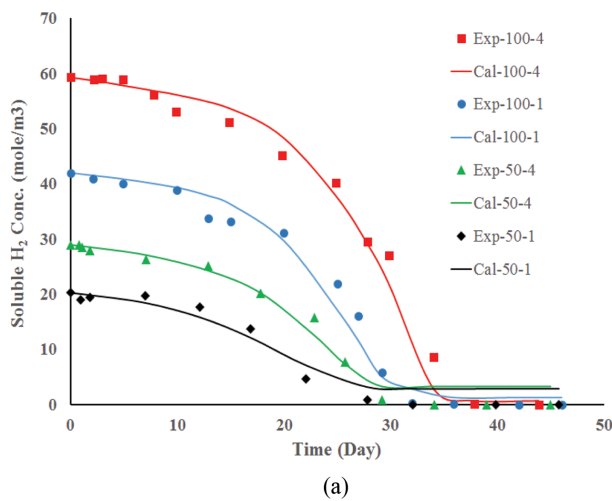


Fig. 2. Prediction of variations in (a) H₂, (b) biomass, (c) CO₂ and (d) CH₄ experimental concentrations (dots) using kinetic modelling equipped with globally optimized kinetic parameters under different experimental conditions of mole ratios of 1 : 1 or 4 : 1 and fixed pressure of 50 or 100 atm [23].

ied on the response using analysis of variance (ANOVA) through a central composite design (CCD). On this basis, five levels for each of the independent variables are considered caused a design of experiment with totally 31 runs. The minimum subsidy value, to achieve a profitable process, should be determined so that the whole of 31 runs gives a positive value. The height to diameter ratio of the bioreactor was fixed at 0.5, as it was previously shown a better geometry configuration than a column bioreactor (height to diameter ratio >1) due to a better expected mass transfer purposes (data unpublished).

The effect of main factors as well as their interactions can be assessed on the process income. In addition, the best configuration of the studied factors for maximizing income can be achieved via RSM, as one of the powerful tools for optimization, in a way that less H_2 and CO_2 are consumed and higher methane is produced.

RESULTS AND DISCUSSIONS

1. Model Evaluation Based on Kinetic Aspect

Different sets of kinetic parameters under a variety of experimental conditions were globally optimized through a predefined procedure, that was previously used for parameter optimization [24]. The finalized kinetic parameters used in Eqs. (2) to (6) are presented in Table 2.

These finalized kinetic parameters are employed in kinetic reaction modelling where H_2 and CO_2 consumption as well as CH_4 and biomass production rates are separately depicted in Fig. 2. According to this figure, significantly good agreement was achieved between the whole experimental data at different conditions and model predictions. Actually, such a conformity verifies reliable parameters for process prediction under the whole range of studied experimental conditions.

It is clear from Fig. 2 that increasing pressure increased the solubility of H_2 and CO_2 in the culture medium, which led to improvement of microorganism growth and consequently CH_4 production. So, increasing pressure can compensate for the slowness of biological reaction to some extent. In addition, it is seen that increasing H_2/CO_2 mole ratio eventually increases methane production. The developed kinetic modelling along with the used procedure for kinetic parameters globalization revealed a satisfying data prediction compared with the reference literature's data fitting [23]. The verified kinetic parameters served within the reaction terms in the following section where mass transfer modelling is developed.

2. Model Evaluation Based on Mass Transfer Aspect

The mass transfer governing equations provided in the methodology section along with their boundary conditions will effectively predict concentration profiles if valid diffusion coefficients are included in the model. Diffusivity coefficients of components in

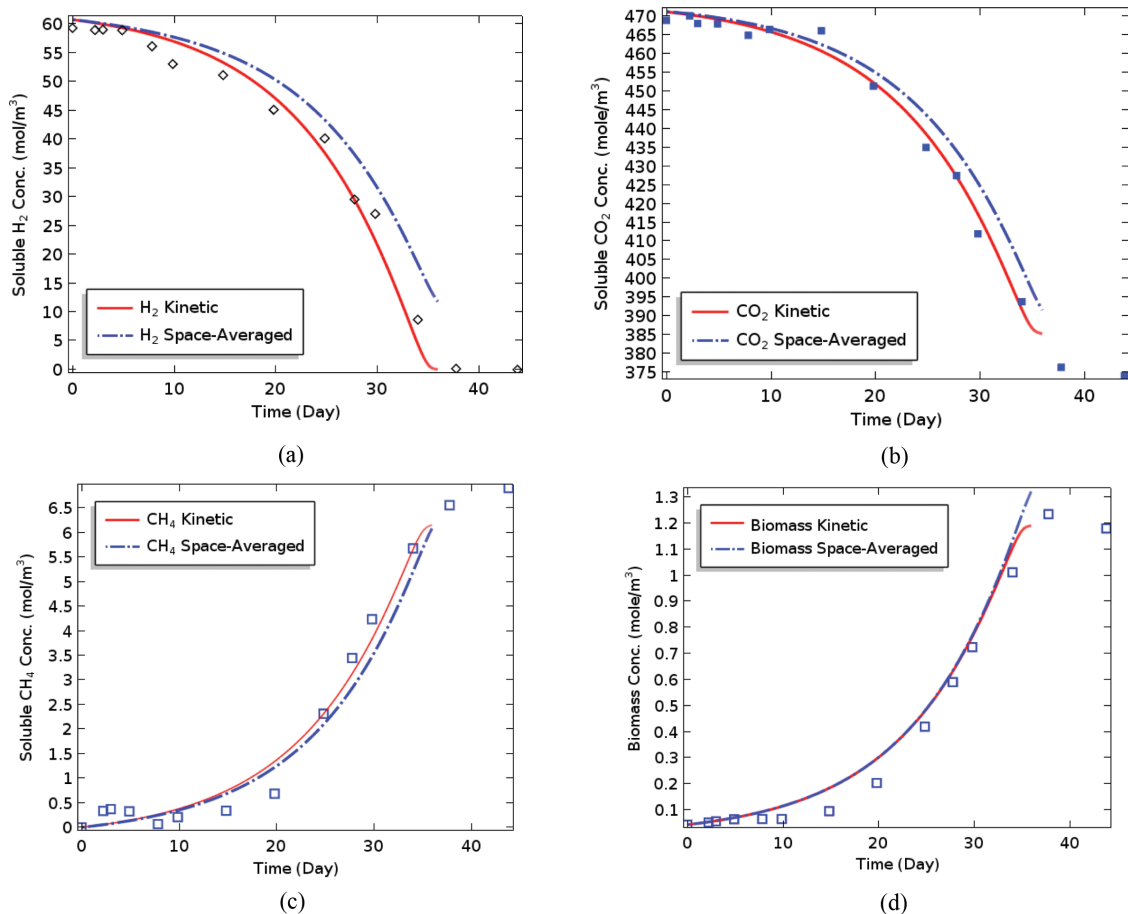


Fig. 3. Comparison of space-averaged concentrations obtained via mass transfer modeling (dashed-line), kinetic (solid line) and experimental data (dots) of (a) soluble H_2 , (b) soluble CO_2 , (c) soluble CH_4 and (d) biomass concentrations.

aqueous phase, $D_{L,p}$, as well as pair component diffusion coefficient in the gas mixture, D_{ij} , were substituted from literature as a function of temperature and pressure as shown in Table A1, Appendix A. Mass transfer model performance was investigated through tracing H_2 , CO_2 , and CH_4 concentrations profiles versus time and the height of the liquid phase of the bioreactor. However, due to lack of experimental data, figures were not illustrated here.

Model verification was carried out using time-dependent experimental data. In this regard, a synchronization was performed by converting space-dependent model results to space-independent ones via averaging soluble component concentrations using Eq. (23) over the length of liquid phase for each single time intervals.

$$C_{L,ave,i} = \frac{\int_{z_L}^{z_g} C_{L,i} dz}{z_g - z_L} \quad (23)$$

where $C_{L,ave,i}$ is the space-averaged concentration of the soluble

component i (H_2 , CO_2 , CH_4 , and biomass) throughout the depth of the liquid phase. Comparative results of $C_{L,ave}$ along with experimental data and kinetic model results are depicted in Fig. 3 over 35 days of running the bioreactor. The experimental conditions were considered fixed at $H_2/CO_2=4$, $P=100$ atm, $T=313$ K, saturated initial concentrations and corresponding diffusion coefficients based on data reported in Table A1.

As seen, space-averaged results in the case of H_2 , CO_2 , CH_4 , and biomass satisfactorily follow the kinetics and experimental data; however, in the case of H_2 concentration, some divergence can be observed between kinetic and space-averaged lines. This can be attributed to H_2 diffusion coefficient in the culture medium, D_{L,H_2} , which was expected to be less than its value in water due to medium impurities. Diffusivity values were assumed in water. Since the kinetic of biomass growth and subsequently methane production depends directly on soluble H_2 concentration, variations in H_2 diffusion coefficient would have major effects on methane concentration. In-

Table 3. Central composite design for evaluating the effect of main factors on the response

Run order	Factors				Response (income)		Residual ($Y_{mod} - Y_{prd}$)
	A	B	C	D	Simulation value ($-Y_{mod}$)	Predicted value ($-Y_{prd}$)	
1	330	100	2.75	0	0.0284	0.0295	-0.0011
2	330	50	2.75	30	0.0132	0.0130	0.0002
3	317.5	125	1.5	45	0.0354	0.0361	-0.0007
4	342.5	125	1.5	15	0.0383	0.0385	-0.0002
5	330	100	2.75	60	0.0200	0.0201	-0.0001
6	330	100	2.75	30	0.0249	0.0248	0.0001
7	317.5	75	4	15	0.0188	0.0185	0.0003
8	330	100	2.75	30	0.0249	0.0248	0.0001
9	342.5	75	1.5	15	0.0229	0.0230	-0.0002
10	317.5	75	1.5	15	0.0263	0.0270	-0.0006
11	317.5	125	4	15	0.0298	0.0300	-0.0002
12	317.5	75	4	45	0.0164	0.0165	-0.0001
13	330	100	2.75	30	0.0249	0.0248	0.0001
14	355	100	2.75	30	0.0223	0.0215	0.0008
15	330	100	2.75	30	0.0249	0.0248	0.0001
16	330	100	2.75	30	0.0249	0.0248	0.0001
17	342.5	125	4	15	0.0262	0.0259	0.0003
18	342.5	125	1.5	45	0.0311	0.0312	-0.0001
19	330	100	0.25	30	0.0378	0.0374	0.0005
20	330	100	2.75	30	0.0249	0.0248	0.0001
21	317.5	125	1.5	15	0.0458	0.0448	0.0010
22	330	100	5.25	30	0.0192	0.0196	-0.0004
23	342.5	75	1.5	45	0.0190	0.0191	-0.0001
24	317.5	125	4	45	0.0250	0.0246	0.0004
25	330	100	2.75	30	0.0249	0.0248	0.0001
26	342.5	125	4	45	0.0223	0.0219	0.0004
27	305	100	2.75	30	0.0289	0.0281	0.0007
28	342.5	75	4	45	0.0153	0.0161	-0.0008
29	342.5	75	4	15	0.0172	0.0168	0.0004
30	330	150	2.75	30	0.0356	0.0366	-0.0010
31	317.5	75	1.5	45	0.0215	0.0216	-0.0001

creasing methane production followed by increasing diffusivity in culture medium was previously discussed by Luo and Angelidaki [31]. Trends shown in Fig. 3 revealed that the optimized kinetic parameters as well as the developed mass transfer modelling are both reliable in process efficiency prediction.

In addition, space-averaged concentrations in the gas phase were calculated in the same way explained in Eq. (23), and concentration profiles, as partial pressure variations, were determined over time (data not shown). However, concentration profiles within the gas phase can be neglected due to the low height of the gas phase.

3. Maximizing Income Using RSM

Upon model verification, income values were calculated for the whole 31 runs corresponding to variety of experimental situations. Using RSM for optimization of a continuous and pressurized biomethanation process was successfully implemented by Leonzio [22].

However, investigating income through the current equation, Eq. (22), is a novel approach that was not found before to the best of our knowledge. Table A2, in Appendix A, reports the corresponding economic values for terms used in calculating income, Eq. (22). By considering a long-term scenario, negative incomes are achieved through the 31 runs. As a basis, a minimum carbon subsidy value equal to \$30/ton CO_2 was considered in Eq. (22), for income calculations. It means that more financial assistance should be provided by the government to have a profitable batch biomethanation process. The achieved results are shown in Table 3. In this table $Y_{mod.}$ and $Y_{prd.}$ are referred to as income values obtained by the mathematical modelling and predicted responses by RSM, respectively. ANOVA reveals that all the studied factors significantly affect income due to corresponding P-values less than 0.05. Based on that, the modified polynomial quadratic model is proposed

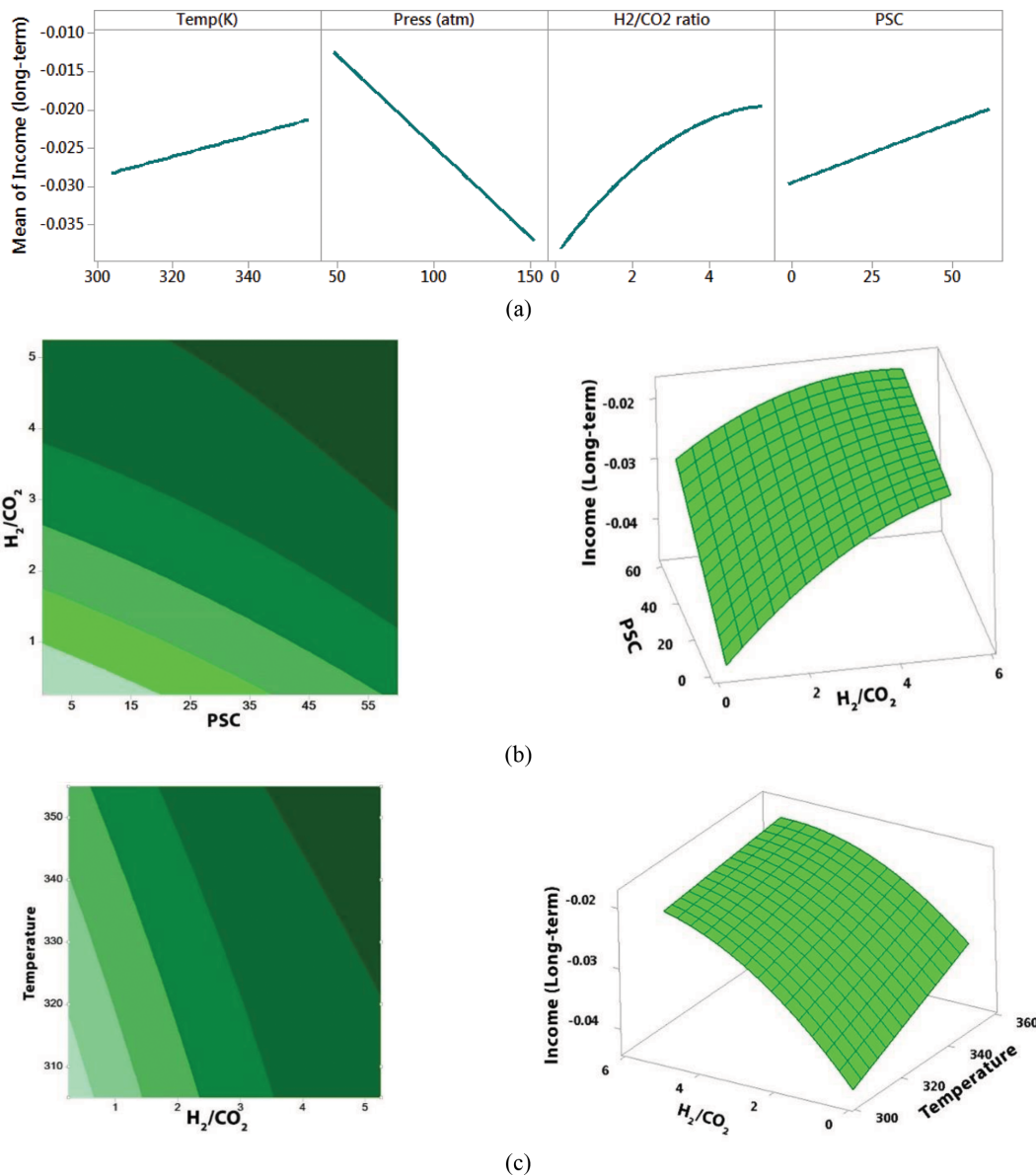


Fig. 4. (a) main effect plots and interaction plots (contour and surface) for (b) H_2/CO_2 with PSC as well as (c) temperature with H_2/CO_2 . Carbon subsidy was considered \$30/ton CO_2 equivalent to carbon tax.

as shown in Eq. (24) via removing insignificant terms (P -value > 0.05).

$$Y_{\text{prod}} = -0.0347 + 0.000096 A - 0.00107 B + 0.0145 C + 0.00068 D - 0.00059 C^2 + 0.000002 A.B - 0.000035 A.C - 0.000002 A.D + 0.000051 B.C + 0.000002 B.D - 0.000044 C.D \quad (24)$$

In addition, ANOVA analysis discloses that all the two-way interactions of factors significantly influence income. It means that the calculated income is influenced by not only one but two factors simultaneously. The high values of $R^2=0.996$ and $\text{adj}R^2=0.993$ suggest a significantly good correlation between data obtained by modeling and data predicted via RSM. Also, the presence of square term regarding the C factor (H_2/CO_2) in the proposed polynomial model implies a curvature in the response function [22]. Statistically, other main factors do not exhibit such curvature. The magnitude and sign of the main coefficients in the polynomial model suggest that H_2/CO_2 has the most influence on the response followed by pressure, PSC and temperature, in the next order of importance. Furthermore, the effect of all main factors except pressure were positive on the response. This implies that increasing pressure diminishes income, while increasing the other factors improve it. Fig. 4 shows the main effect plots as well as contour and surface plots for investigating interaction effects of H_2/CO_2 , temperature and PSC.

All the trends seen in Fig. 4 are mathematically justifiable and all demonstrated under the lowest carbon subsidy of \$30/ton CO_2 . As seen in Fig. 4(a), increasing temperature increases income or decreases financial loss. According to the gas law, at a given pressure, higher temperatures cause a lower concentration of components in the gas phase, which means less money should be paid for providing substrate. This is while the money gained via selling the produced amount of methane makes income positive. So, the process efficiency improves and a lower financial loss can be expected at higher temperature when only \$30/ton carbon subsidy is dedicated. It is worth mentioning that a high-temperature bi-methanation process would be possible if only thermophilic methanogens were used at temperature range of 320 up to 350 K [32]. Otherwise, the process would fail. Meanwhile, temperature rising cost should be taken into account.

Based on Fig. 4(a), increasing pressure decreased income or, in the other words, increased financial loss. Although higher pressure increases gas solubility in water as well as component concentration in the gas phase, more money should be expended for purchasing gaseous substrates, H_2 and CO_2 . This is while the amount of produced methane is not enough to compensate it. Therefore, low-pressure bi-methanation process would be more attractive based on the gained modeling results. Note that under lower pressures the possibility of increasing acidity of medium due to CO_2 solubility would be decreased. The issue should be considered in the case of running the bi-methanation process in an underground high pressure natural reservoir.

According to the stoichiometry of the methanation reaction, Eq. (1), a mole ratio of $H_2/CO_2=4$ should be supplied to the bioreactor to achieve one mole of methane. Fig. 4 implies that more favorable economic condition arises at higher substrates mole ratios, and its exact value was achieved 3.98 based on RSM response optimizer. However, this variation is not linear.

In the case of PSC factor, it was found that it should be supplied in a maximum value to have maximum income. Fig. 4(a) and (b) show that the calculated income improves almost linearly with PSC. It means providing initially soluble gaseous substrate in the medium motivates more biomass growth and metabolic activity rather than supplying the substrate only through diffusion from the gas phase. Indeed, larger volume of microorganisms is involved in the batch bi-methanation process when microorganisms are supplemented with high PSC. While, running the process under substrate diffusion from the top phase promotes only surface microorganisms in methane production.

It was found from response optimizer that if the near-term scenario is considered for bi-methanation process, the amount of achieved income is 36% higher than that of long-term scenario. According to Table A2, in appendix A, benchmark capture cost for near-term scenario is about \$36.63/ton CO_2 .

In addition, the minimum subsidy which can be supplied by the government to achieve a profitable process under the whole of 31 runs should be at least \$363/ton CO_2 and \$327/ton CO_2 for long- and near-term scenarios, respectively. Therefore, a bi-methanation plant which is working under a batch process does not come to profit unless receiving at least 12-fold or 11-fold subsidy more than an average CO_2 tax (\$30/ton CO_2), respectively. Otherwise, the produced bi-methane should be sold for nearly \$34,000/ton CH_4 , which is undoubtedly unaffordable.

4. Sensitivity Analysis

The sensitivity of income against some controllable process parameters such as height over diameter of the bioreactor (H_L/D), D_L , gas volume (V_g), liquid volume (V_L), pressure, temperature, and PSC was evaluated and results presented in Fig. 5. The bio-kinetic parameters are not considered as controllable parameters as they vary only by microorganism strain or substrates substitution [33]. All the parameters were kept constant during sensitivity analysis except that of concern. In addition, the effect of all the considered factors was investigated under a vast range of possible carbon subsidies from 30 to \$300/ton CO_2 . According to Fig. 5, the carbon subsidy plays a prominent role concomitant with process parameters in financial investigations of a batch bi-methanation process.

As seen in Fig. 5(a), increasing liquid height to diameter ratio of the bioreactor (H_L/D) from 0.1 to 8.5 positively influences the calculated income when \$30 carbon subsidy is allocated to the process per ton of CO_2 . However, increasing the carbon subsidy up to \$300/ton CO_2 caused a reverse trend in which more income can be expected in a flat bioreactor with lower H_L/D . Although it was found from previous research data that a wider bioreactor facilitates mass transfer (data unpublished), financial consideration in the present study reveals that a column-shaped bioreactor would be affordable in total. Indeed, gaseous substrate consumption would be higher in a flat bioreactor than that of a column type.

Fig. 5(b) shows that liquid diffusivity coefficient, D_L , negatively affects the income in the case of low subsidy. D_L can be considered as gentle liquid mixing. Increasing D_L from a magnitude of 10^{-9} to 10^{-6} caused a 70% drop in the income or, in the other words, a 70% rise in financial loss. Increasing D_L caused more gaseous substrate to be solubilized in the liquid medium, which led to increased expenses. This is while, the produced methane is not that much to

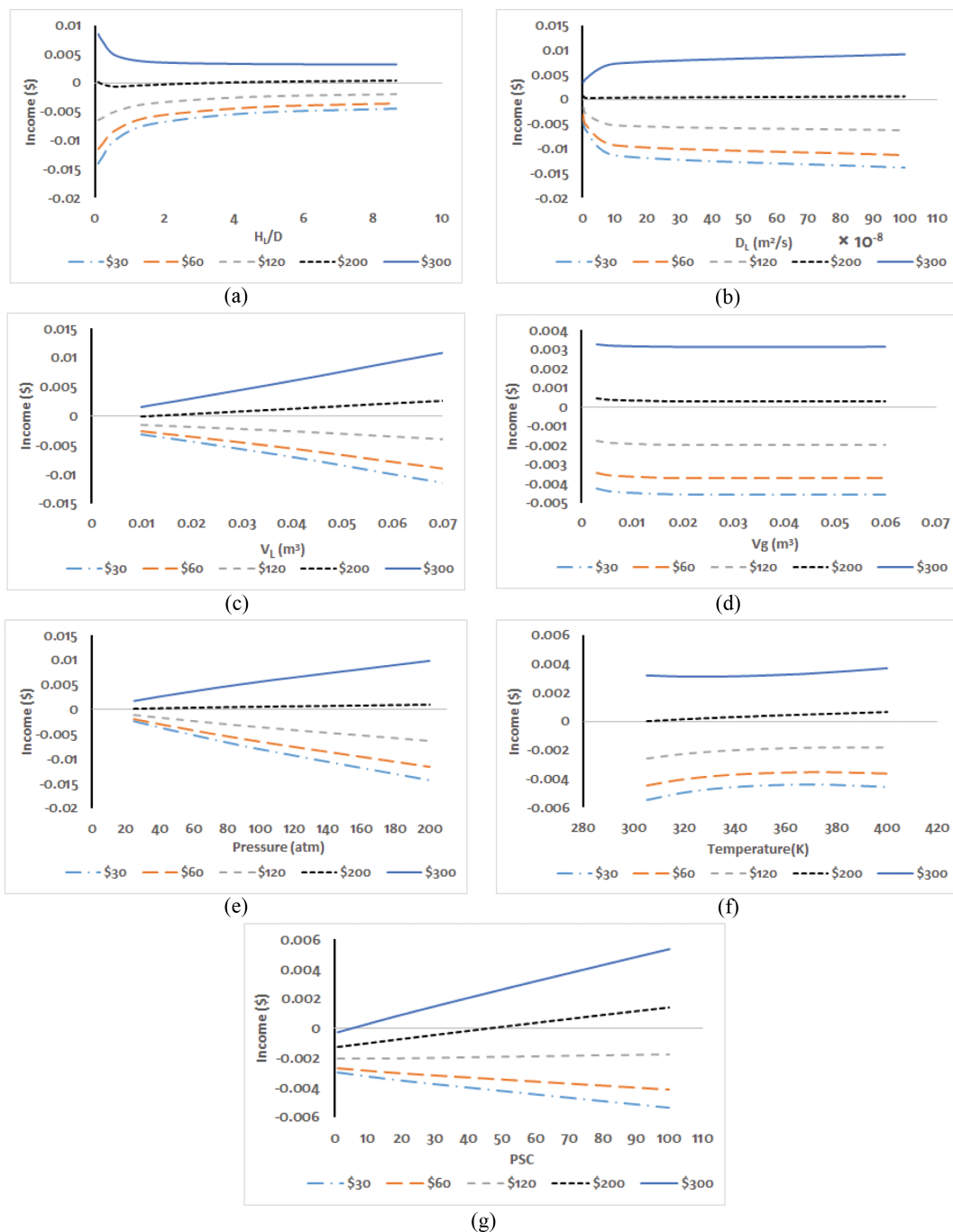


Fig. 5. Sensitivity analysis for investigating the effect of (a) H_L/D , (b) D_L , (c) V_L , (d) V_g , (e) pressure, (f) temperature and (g) PSC on income under carbon subsidies from 30 to \$300/ton CO_2 .

economically compensate such deficiency. In the case of carbon subsidies higher than \$200/ton CO_2 , higher D_L values are more welcomed. Also, there is no liquid mixing in the case of performing the biomethanation process in an underground natural gas reservoir.

Sensitivity of income for V_L and V_g variations is seen in Fig. 5(c) and 5(d). When low levels of carbon subsidy are dedicated to the process, increasing V_L , at a fixed V_g , negatively and almost linearly decreases the income; however, the trend becomes positive only if the subsidy gets around \$200/ton CO_2 . Based on Fig. 5(d), increas-

ing the gas volume, V_g , under a fixed pressure and V_L , nonlinearly decreases income in the whole range of studied carbon subsidies from 30 to \$300/ton CO_2 . Higher subsidies should be considered to achieve a positive income. According to Fig. 5(e), pressure imposes the same effect as V_L on income. It means that increasing pressure linearly decreases the calculated income under low carbon subsidies, which is in the line with RSM results (Fig. 4(a)). If the government creates more incentives on carbon consumption, the batch biomethanation process would be more attractive at higher

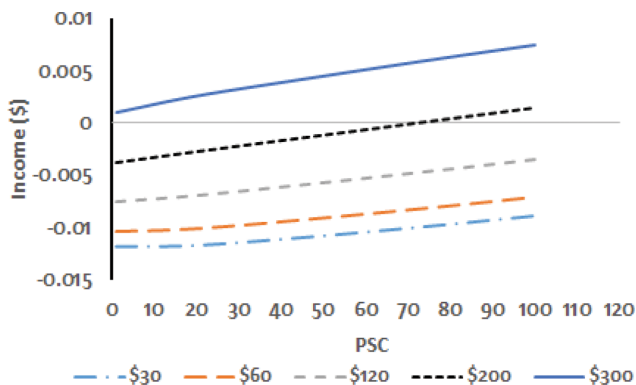


Fig. 6. Sensitivity analysis for PSC in a flat bioreactor with $H_L/D=0.5$ and carbon subsidy variations between 30 to \$300/ton CO_2 .

pressures. Therefore, implementing the biomethanation reaction as a batch process in an underground reservoir, with high intrinsic pressures, might be uneconomical with carbon subsidies lower than \$200/ton CO_2 if the other terms in Eq. (22) are assumed to be constant.

In the case of process temperature, it shows a bell-shaped effect on the calculated income. Fig. 5(f) illustrates that increasing the temperature from 305 to 400 K initially increased the income and then decreased it at around 370 K, when the carbon subsidy was fixed as low as \$30/ton CO_2 . It is in compliance with the obtained results by RSM for temperature, Fig. 4(a). Indeed, raising more the temperature improves gas solubility in water due to lowering Henry's constant of the participant gas [30]. However, allocating more subsidy up to \$300/ton CO_2 caused a reversed bell-shape with a minimum peak value around 320 K.

Fig. 5(g) illustrates the effect of PSC on the income. The same trend as pressure is seen under the entire range of low and high car-

bon subsidies. Increasing PSC means that higher costs should be paid for providing initial gaseous substrates in the culture medium. However, as seen, allocating more subsidies than \$120/ton CO_2 may gradually turn the trend and make the process more economic at higher PSC.

Comparing Fig. 4(a) and Fig. 5(g) with low level of subsidy reveals that there is a mismatch between PSC trends found by RSM and sensitivity analysis: meanwhile, the H_L/D value was fixed at 0.5 and 2, respectively. Fig. 6 discloses that the value of H_L/D parameter determines the obtained trends. Indeed, a wide bioreactor with $H_L/D=0.5$ gives significantly different trends of PSC compared to that achieved by $H_L/D=2$ (Fig. 5(g)).

With a glance at Fig. 6, it is clear that income has a positive relationship with PSC at low and high levels of carbon subsidy, unlike that found in Fig. 5(g). Therefore, Fig. 6 verifies the results of PSC found by RSM illustrated in Fig. 4(a). Changing H_L/D imposed no significant variations in trends of the other factors investigated in Fig. 5.

To inform of the most effective process parameters with the highest income results, Fig. 7 is depicted. It contains a comparative view of the most significant levels of each of the studied parameters under both subsidies of 30 and \$300/ton CO_2 .

It is clear from Fig. 7 that, if low subsidy is dedicated to the process, the factors pressure, PSC(8.5), V_L , D_L , V_g , H_L/D , PSC(0.5) and temperature will achieve highest incomes, respectively. However, when the biomethanation process meets circumstances to have higher subsidy of \$300/ton CO_2 , the most important parameters would be V_L , pressure, D_L , H_L/D , PSC(0.5), temperature, PSC(8.5) and V_g , respectively.

CONCLUSION

As a challenging issue, gas/liquid mass transfer in a batch bio-

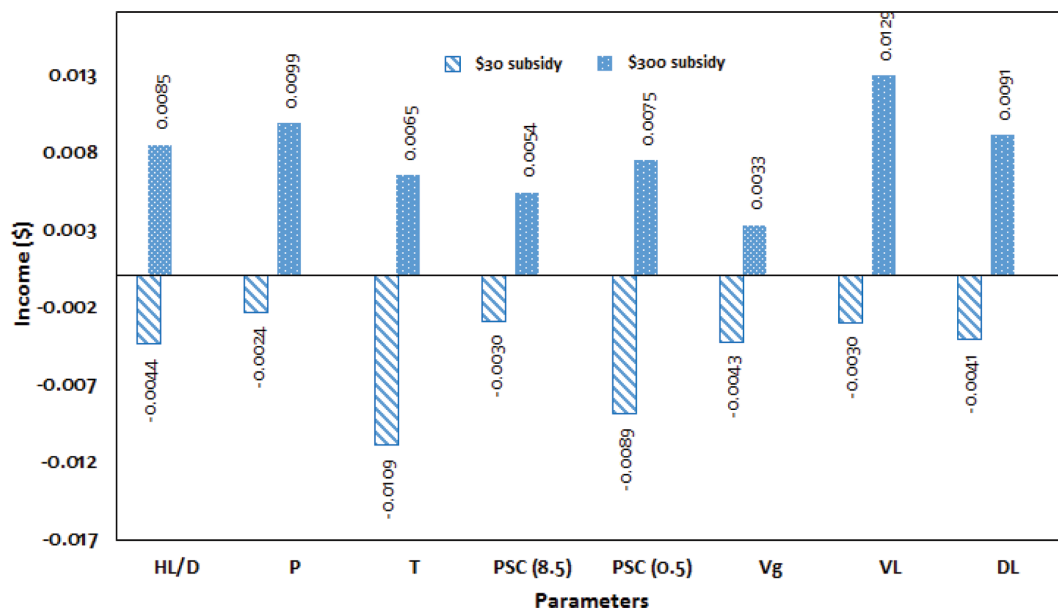


Fig. 7. Comparative view of the most significant levels of each of the studied factors under both subsidies of 30 and \$300/ton CO_2 . PSC(8.5) and PSC(0.5) are those obtained with $H_L/D=8.5$ and 0.5, respectively.

methanation reactor should be precisely taken into account. This paper addressed the issue through kinetic and mass transfer modelling to achieve substrates, product, and biomass concentration profiles versus time and space within both gas and liquid phases of the bioreactor. As a prerequisite, six unknown kinetic parameters were globally optimized via a predefined algorithm. The values of 0.09872 day⁻¹, 1.54222, 0.13740 day⁻¹, -0.01830, -1.36359, and -0.09077 were obtained in this way for the corresponding kinetic parameters of μ_{max} , k_L , m , $Y_{X/L}$, $Y_{C/L}$, and $Y_{P/L}$, respectively. Then, mass transfer modelling was developed and the space-averaged (space-independent) results were verified via some space-independent experimental data. The developed model was utilized to predict the amount of consumed and produced gases over time and subsequently the process income. As a novelty of the current study, an equation was proposed to calculate process income based on the amount of consumed and produced gases as well as considering a term for carbon subsidy. Then RSM design of experiment was conducted to investigate the effect of four independent variables: H₂/CO₂, PSC, temperature, and pressure on the studied response, income. It was found that highest levels of temperature and PSC as well as lowest level of pressure and H₂/CO₂=3.98 led to achieve maximum income. However, a break-even income would be achieved if only a carbon subsidy of \$363/ton CO₂ is allocated to the process. Sensitivity analysis revealed that the amount of carbon subsidy significantly influenced on the positive or negative trends of the studied factors versus the calculated income. On this basis, pressure was the most important factor to achieve maximum income when a low carbon subsidy of \$30/ton CO₂ is allocated to the process. This is while, both V_L and pressure were found as the most important factors to have maximum income in the case of higher subsidies of \$300/ton CO₂. Evidences suggested that implementation a batch biomethanation process in an underground gas reservoir with intrinsic high pressure and temperature as well as large surface area (low H_L/D), due to porosity, would be affordable if only large amount of carbon subsidy is assigned to the process.

NOMENCLATURE

C_{Lini} : initial concentration in liquid phase [mole·m⁻³]
 C_{gini} : initial concentration in gas phase [mole·m⁻³]
 \bar{D}_{ij} : multicomponent Fick diffusivity [m²·s⁻¹]
 C_L : time and space dependent concentration in the liquid phase [mole·m⁻³]
 $C_{L,ave}$: space-averaged concentration in liquid phase [mole·m⁻³]
 C_{Ls} : liquid concentration on gas-liquid interface [mole·m⁻³]
 C_X : time and space dependent concentration of biomass [mole·m⁻³]
 C_g : time and space dependent concentration in gas phase [mole·m⁻³]
 $C_{g,ave}$: space-averaged concentration in gas phase [mole·m⁻³]
 C_{gs} : gas concentration on gas-liquid interface [mole·m⁻³]
 $D_{L,i}$: diffusivity coefficient of gases in liquid phase [m²·s⁻¹]
 $D_{eff,i}$: effective diffusion coefficient of component i in gas mixture [m²·s⁻¹]
 D_i^T : thermal diffusion coefficient
 D_{ij} : diffusion coefficient of pair gases [m²·s⁻¹]

N_L : liquid diffusive flux [mole·m⁻²·s⁻¹]
 N_g : gas diffusive flux [mole·m⁻²·s⁻¹]
 $Y_{i/L}$: theoretical maximal (C)-molar yields on the basis of hydrogen
 Y_{mod} : response value obtained via modelling
 Y_{prd} : response value predicted by RSM
 k_L : saturation constant [mole·m⁻³]
 q_L^{max} : maximum H₂ consumption [mole·m⁻³]
 r_{H_2} : H₂ consumption rate [mole·m⁻³·s⁻¹]
 r_C : CO₂ consumption rate [mole·m⁻³·s⁻¹]
 r_P : CH₄ production rate [mole·m⁻³·s⁻¹]
 r_X : biomass growth rate [mole·m⁻³·s⁻¹]
 y_j : mole fraction in gas phase
 ω_j : mass fraction
 ∇P : pressure gradient
 ∇T : temperature gradient
 H_r : dimensionless Henry's constant
 m : microorganism maintenance coefficient [day⁻¹]
 u : velocity [m·s⁻¹]
 ρ : mixture density [Kg·m⁻³]
 μ_{max} : maximum growth rate of biomass [day⁻¹]

REFERENCES

1. C. Ampelli, S. Perathoner and G. Centi, *Philos. Trans. R. Soc. A*, **373**, 20140177 (2015).
2. C. Steinlechner and H. Junge, *Angew. Chem. Int. Ed.*, **57**, 44 (2018).
3. J. G. Olivier and J. Peters, *Trends in global CO₂ and total greenhouse gas emissions*, Report (2018).
4. B. Dudley, *BP statistical review of world energy*, Report (2018).
5. Q. Chai, Z. Xiao, K.-h. Lai and G. Zhou, *Int. J. Prod. Econ.*, **203**, 311 (2018).
6. H. Naims, *Environ. Sci. Pollut. Res.*, **23**, 22226 (2016).
7. M. Bailera, P. Lisbona, L. M. Romeo and S. Espotolero, *Renew. Sust. Energy Rev.*, **69**, 292 (2017).
8. G. Iaquaniello, S. Setini, A. Salladini and M. De Falco, *Int. J. Hydrogen Energy*, **43**, 17069 (2018).
9. J. Squalli, *Energy*, **127**, 479 (2017).
10. H. Blanco, W. Nijs, J. Ruf and A. Faaij, *Appl. Energy*, **232**, 323 (2018).
11. J. H. Kim, W. S. Chang and D. Pak, *Korean J. Chem. Eng.*, **32**, 2067 (2015).
12. E. Inkeri, T. Tynjälä, A. Laari and T. Hyppänen, *Appl. Energy*, **209**, 95 (2018).
13. K. Ghail and F.-Z. Ben-Fares, *Renew. Sust. Energy Rev.*, **81**, 433 (2018).
14. R. Tarkowski, *Renew. Sust. Energy Rev.*, **105**, 86 (2019).
15. S. Savvas, J. Donnelly, T. Patterson, Z. S. Chong and S. R. Esteves, *Appl. Energy*, **202**, 238 (2017).
16. J. Biswas, R. Chowdhury and P. Bhattacharya, in *Industry interactive innovations in science, engineering and technology*, S. Bhattacharyya, S. Sen, M. Dutta, P. Biswas and H. Chattopadhyay Eds., Springer, Singapore (2018).
17. I. Diaz, C. Perez, N. Alfaro and F. Fdz-Polanco, *Bioresour. Technol.*, **185**, 246 (2015).
18. W. Merkle, K. Baer, J. Lindner, S. Zielonka, F. Ortloff, F. Graf, T. Kolb, T. Jungbluth and A. Lemmer, *Bioresour. Technol.*, **232**, 72 (2017).

19. D. Strubing, B. Huber, M. Lebuhn, J. E. Drewes and K. Koch, *Biore-sour. Technol.*, **245**, 1176 (2017).
20. Y. Huang, F. Mahmoodpoor-Dehkordy, Y. Li, S. Emadi, A. Bagtzoglou and B. Li, *Chem. Eng. J.*, **334**, 1383 (2018).
21. A. Bensmann, R. Hanke-Rauschenbach, R. Heyer, F. Kohrs, D. Bendorf, U. Reichl and K. Sundmacher, *Appl. Energy*, **134**, 413 (2014).
22. G. Leonzio, *Chem. Eng. J.*, **290**, 490 (2016).
23. J. Y. Leu, Y. H. Lin and F. L. Chang, *Chem. Eng. Res. Des.*, **89**, 1879 (2011).
24. S. Osfouri and R. Azin, *Gas Process.*, **4**, 14 (2016).
25. W. Hayduk and H. Laudie, *AIChE J.*, **20**, 611 (1974).
26. D. Fairbanks and C. Wilke, *Ind. Eng. Chem.*, **42**, 471 (1950).
27. T. R. Marrero and E. A. Mason, *J. Phys. Chem. Ref. Data*, **1**, 3 (1972).
28. S. Weissman and G. Dubro, *J. Chem. Phys.*, **54**, 1881 (1971).
29. T. Chu, P. S. Chappellear and R. Kobayashi, *J. Chem. Eng. Data*, **19**, 299 (1974).
30. R. Fernández-Prini, J. L. Alvarez and A. H. Harvey, *J. Phys. Chem. Ref. Data*, **32**, 903 (2003).
31. G. Luo and I. Angelidaki, *Biotechnol. Bioeng.*, **109**, 2729 (2012).
32. J. Zabranska and D. Pokorna, *Biotechnol. Adv.*, **36**, 707 (2018).
33. J. Owens and J. Legan, *FEMS Microbiol. Rev.*, **3**, 419 (1987).
34. S. P. Cadogan, G. C. Maitland and J. M. Trusler, *J. Chem. Eng. Data*, **59**, 519 (2014).
35. J. W. Schmelzer, E. D. Zanutto and V. M. Fokin, *J. Chem. Phys.*, **122**, 074511 (2005).
36. M. D. Rosa, *Energy Environ.*, **31**, 60 (2018).
37. G. Glenk and S. Reichelstein, *Nat. Energy*, **4**, 216 (2019).

APPENDIX A

Table A1. $D_{L,i}$ and D_{ij} used in the mass transfer model at temperature of 313 K and working pressures of 50 and 100 atm

	$D_{L,i} \text{ (m}^2\text{/s)} \times 10^{-9}$		Reference	$D_{ij} \text{ (m}^2\text{/s)} \times 10^{-5}$		Reference	
	50 ^a atm	100 ^b atm		50 atm	100 atm		
D_{L,CO_2}	2.541	2.537	[25,34]	D_{CH_4,CO_2}	0.036	0.018	[27,28]
D_{L,CH_4}	2.084	2.081	[25]	D_{CH_4,H_2}	2.596	1.198	[27,29]
D_{L,H_2}	6.279	6.267	[25]	D_{H_2,CO_2}	0.141	0.070	[27]

Water viscosities at temperature of 313 K and pressures of ^a50 atm and ^b100 atm were interpolated as 0.6502 and 0.6513 cP, respectively [35].

Table A2. Values for terms used in Eq. (22)

Terms	Value (\$/ton)	Comment	Reference
Upgraded biomethane price	1158.25	-	[36]
CO ₂ capture cost	36.63	Near-term scenarios with small scale high purity CO ₂ utilization and low benchmark capture cost	[6]
	72.15	Long-term scenario with large scale CO ₂ utilization and higher benchmark capture cost	
CO ₂ tax	30	Average in Europe	-
Renewable H ₂ cost	3585.3	Break-even prices in Germany	[37]